Granatier, Marianna; Lê, Huy Quang; Ma, Yibo; Rissanen, Marja; Schlapp-Hackl, Inge; Diment, Daryna; Zaykovskaya, Anna; Pokki, Juha-Pekka; Balakshin, Mikhail; Louhi-Kultanen, Marjatta; Alopaeus, Ville; Sixta, Herbert

Gamma-valerolactone biorefinery: Catalyzed birch fractionation and valorization of pulping streams with solvent recovery

Gamma-valerolactone biorefinery: Catalyzed birch fractionation and valorization of pulping streams with solvent recovery

Marianna Granatier [a], Huy Quang Lê [a], Yibo Ma [a], Marja Rissanen [b], Inge Schlapp-Hackl [a], Daryna Diment [a], Anna Zaykovskaya [c], Juha-Pekka Pokki [c], Mikhail Balakshin [a,1], Marjatta Louhi-Kultanen [c], Ville Alopaeus [c], Herbert Sixta [a,*]

[a] *School of Chemical Engineering, Department of Biosystems and Bioproducts, Aalto University, Vuorimiehentie 1, 02150, Espoo, Finland*
[b] *Department of Materials Science, University of Tampere, Kuntokatu 3, 33520, Tampere, Finland*
[c] *School of Chemical Engineering, Department of Chemical and Metallurgical Engineering, Aalto University, Vuorimiehentie 1, 02150, Espoo, Finland*

ABSTRACT

In this study, we propose a full gamma-valerolactone (GVL) organosolv biorefinery concept including the utilization of all pulping streams, solvent recovery, and preliminary material and energy balances. GVL is a renewable and non-toxic solvent that fractionates woody biomass. The silver birch chips were pulped (45–65 wt% GVL, 150 °C, 2 h) under a series of acid-catalyzed conditions (5–12 kg H_2SO_4/t), and the fully bleached pulp was spun into fibers by the ION-CELL® process and knitted into the fabric. The dissolved lignin was precipitated by water from spent liquor (1:1) and processed into polyhydroxyurethane. Most of the dissolved hemicelluloses were in the form of xylose, therefore, the crystallization efficiency of xylose from spent liquor in the presence of residual GVL was studied. The GVL recovery rate in the lab column was 66%, however by increasing the number of equilibrium stages, 99% recovery could be achieved.

1. Introduction

The Agenda for Sustainable Development 2030 lists climate change as one of the biggest challenges to combat in today's world [1]. A significant increase in climate temperature is caused to a big extent by the greenhouse gas CO_2 released during the combustion of crude oil [2]. However, fossil reserves represent a major commodity that is relatively inexpensive and readily available to produce platform chemicals of everyday need. As this strong dependency on oil and concerns about climate change intensify across the globe, the interests shift toward renewable feedstock.

Biorefinery is analogous to petrochemical refining, but instead of oil, the conversion of renewable materials into biobased chemicals and fuels takes place. Namely lignocellulosic biomass is believed to be the only renewable carbon source that could compete and replace crude oil thanks to its composition. Despite the simple structure (glucose units connected by β-1,4-glycosidic bonds), cellulose offers special properties like strength, insolubility in water, hydrophilicity, or resistivity to chemical derivatization. Hemi-celluloses are heteropolysaccharides that structurally support the plant, but their chemical and thermal stability are lower than that of cellulose. Lignin, structurally rich in aromatic and aliphatic moieties, provides hydrophobicity and stiffness by gluing cellulose and

---

hemicellulose together. Resins are isolated with different solvents as extracts; typically starting with very hydrophobic solvents such as diethyl ether, moving through acetone or dichloromethane to more hydrophilic solvents such as ethanol (Henriksson and Lennholm 2009; Teleman 2009; Henriksson 2009; Björklund Jansson and Nilvebrant 2009). However, to be economically competitive in the market, a proper technology allowing full utilization of these components is a must.

Currently, acid sulfite (AS) and prehydrolysis kraft (PHK) pulping constitute the most common biorefining of lignocellulosic biomass. Dissolving pulp, the major product of a pulp mill, is predominantly produced by PHK cooks. Although PHK cooks are insensitive to different wood species, yield high-quality pulps, and the pollution prevention is well designed, the process suffers from significant limitations. PHK requires very high investment costs and while steam prehydrolysis complicates the implementation of a biorefinery concept, water prehydrolysis is technically challenging. The AS pulping is the only relevant biorefinery on a commercial scale (Lenzing, Domsjö, or Borregaard plant being examples). However, AS is limited only to certain wood species, the investments to reduce waste-water emissions are high and the sulfur recovery is low. An alternative pulping process must take into the account low consumption of chemicals and their simple recovery, a wide raw material selection, and low energy inputs [3,4].

Organosolv pulping is an organic solvent-based process that represents one technological approach of a modern biorefinery. The basic sulfur-free process combines organic solvent and water where the former promotes lignin dissolution (a major benefit of organosolv) and the latter hydrolysis of hemicelluloses. In addition, the lower viscosity of the organic solvent enables better removal of lignin and reduces its recondensation due to the buffering effect of the produced or added acids, resulting in better bleachability of organosolv pulps compared to kraft pulps [5]. Based on this relatively simple principle, Kleinert and Tayenthal introduced the first successful organosolv cook in the mixture of ethanol and water [6], which was developed over the years into a pilot scale named ALCELL®. Since then, several organic solvents were proposed, such as acetic acid (Acetocell), formic acid (Formacell), performic acid (MILOX), or methanol (Organocell). Many of these proposals failed to cover all the requirements of a sustainable biorefinery. However, more recent advancements including organic solvent gamma-valerolactone or ternary systems SO_2-ethanol-water (SEW) and Clean Fractionation (methyl isobutyl ketone-ethanol-water) sparked interest in the pulping field [7–9]. Although none of the organosolv processes is commercialized yet, Bio2X process based on Chempolis organosolv technology is currently in the pilot phase [10,11].

Gamma-valerolactone (GVL) is a well-known food and cosmetic additive but in biomass fractionation, GVL is a new term. Firstly, described as a sustainable liquid for fuel production, GVL is a lactone exhibiting exceptional physical and chemical properties: non-toxicity, low volatility, and high solubility in water without the formation of an azeotrope [12]. In the presence of a solid acid catalyst, GVL solubilizes cellulose allowing the production of levulinic acid, which can be converted back to GVL by hydrogenation [13]. GVL is a highly stable compound in a wide range of process conditions including extreme pH and high temperatures but a small amount readily hydrolyzes into 4-hydroxyvaleric acid [14]. In the pulping process, GVL acts as a potent lignin solvent in biomass fractionation.

The idea of wood fractionation in GVL was gradually developed. Luterbacher et al. (2014) [15] reported acid-catalyzed pretreatment of carbohydrates in aqueous 70% GVL and non-enzymatic conversion into monomeric glucose and xylose. Fang and Sixta (2015) [16] suggested GVL/water mixture for the sawdust fractionation to obtain pulp together with lignin and dissolved hemicellulose fraction. Shortly after, Lê et al. (2016) proposed the first concept of GVL biorefinery, optimizing the uncatalyzed cooking conditions for eucalyptus wood chips. The cellulose fraction obtained from 50% GVL cook was upgraded into textile fibers, while the valorization of lignin and hemicellulose fraction was debated. In a subsequent study, Lê et al. (2018) investigated in-depth GVL recovery from spent liquor by simple distillation or CO_2 extraction in batch mode. Alonso et al. (2017) presented the most elaborated GVL biorefinery concept in current literature where white birch wood was fractionated in 70% GVL with the addition of sulfuric acid to yield fully bleached pulp. While isolated lignin was used in the production of battery anodes and carbon foam, the hemicelluloses were converted to furfural. The techno-economic evaluation concludes the biorefinery concept [19]. Recent comprehensive work of Talebi et al. (2019) pioneered with an aldehyde-stabilization technology, operating at relatively low temperatures and pressures in the presence of sulfuric acid. In the process, the extraction of uncondensed lignin during fractionation, which can be readily dissolved in an organic solvent while simultaneously producing a relatively pure cellulose fraction, is enhanced [20].

Building on previous knowledge, this paper proposes the possible direction of a modern GVL biorefinery including comprehensive biomass valorization and GVL recovery by liquid CO_2 extraction in continuous mode. Fig. 1 outlines the simplified flow diagram of the
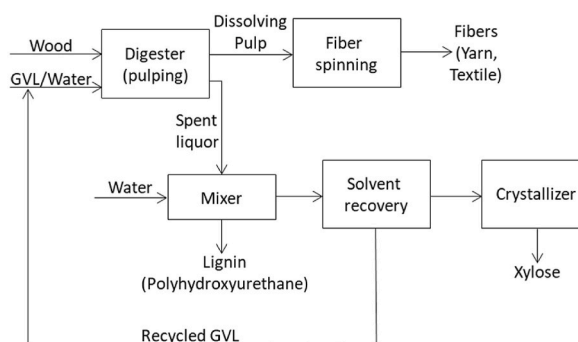

Fig. 1. Flow diagram of proposed processes and main streams.

processes and streams described in this paper. In addition, it analyzes numerous aspects of a potential process including preliminary energy and mass balances. To our knowledge, the presented work on GVL fractionation is so far the only one allowing all polymer fractions of wood (cellulose, hemicellulose, and lignin) to be added to the value chain.

We focused on the production of the platform and bulk materials, rather than on specific high-value chemicals, which might be economically more attractive, but their manufacturing cost would likely exceed their current market price. The following lines describe our motives behind the choices of valorized materials.

The chemical pulp produced via chemical pretreatment is undoubtedly the largest and the most important fraction of a pulp mill with its yearly production exceeding 126 Mt in 2020 [21]. Typically, chemical pulps are classified as paper- or dissolving-grade and their applications range from graphic paper and hygienic products to specialty papers and regenerated fibers. Especially the demand for dissolving pulp known for its high purity (>90% of α-cellulose content) experienced a boom in recent years (10 Mt in 2021) [22]. Therefore, fully bleached dissolving pulp was the first product in our biorefinery line including a detailed characterization of pulps and spent liquor, but the process conditions could be easily customized to produce paper-grade pulp [23].

Fully bleached dissolving pulp was upgraded into regenerated fibers, which are produced predominantly by viscose or Lyocell process. Although both processes are widely established, they are not free from environmental risks. In our biorefinery concept, we opted to upgrade GVL-dissolving pulp using the emerging technology Ioncell® (currently in the pilot phase). Ioncell® is a Lyocell-type process that dissolves cellulose directly in a non-imidazolium-based ionic liquid. Dissolved and filtered cellulose (dope) is extruded through the spinneret, stretched into an air gap, and regenerated in water [24]. Produced fibers were spun into yarn and woven into demonstration fabric.

Besides the pulp, spent liquor composed mostly of lignin and dissolved sugars represents a huge market opportunity. As for lignin, its estimated yearly production falls between 50 and 60 Mt out of which only 2% is commercially used and the rest is incinerated in a recovery boiler [25]. Most of the commercial lignin originates from acid sulfite pulping (lignosulphonates) or kraft pulping. Although the industrial use of lignin is limited due to the chemical and structural heterogeneity leading to the high reactivity of lignin and decreased control over desirable reactions, some of the current applications of lignosulphonates include mostly adhesives and dispersants in construction material. However, advanced research explores the lignin use in for example polyurethanes or carbon fibers [25,26]. Namely, the polyurethane industry generated a revenue of more than 60 billion USD in 2021 and it is predicted to grow [27]. In our GVL biorefinery proposal, we suggest the use of GVL-lignin as a polyol (reinforcing) substrate in polyurethane production.

Dissolved hemicelluloses are the third major byproduct of a pulp mill with approximately 15 Mt production of hemicelluloses yearly. While the hemicelluloses are burned in the industrial process, most of the research focuses on their upgrade into ethanol or furfural. Especially the latter is obtained from pentoses, particularly xylose, by dehydration [25]. Although xylose as such does not get the same attention, it is a valuable chemical precursor in the food and pharmaceutical industry. Therefore, we propose the isolation of monomeric xylose from spent liquor by cooling crystallization.

To our knowledge, the current manuscript is the first one to present a comprehensive study on a) practice-based pulping including detailed and systematic characterization of pulps and liquid streams; b) the practical recovery of wood by-products (cellulose, lignin, and hemicellulose) and their detailed characterization; c) valorization of wood by-products into products of everyday use such as textiles, polyhydroxyurethane, and xylose including a detailed characterization of these items. In addition, for the first time in literature, we present an efficient and novel GVL recovery employing continuously operated CO_2 extraction that was performed in the laboratory extractor, and the experimental results were validated by Aspen simulation. The individual processes in the proposed GVL biorefinery were designed and studied in one sequence, meaning every subsequent step follows the outcomes and results of the previous one. We would like to emphasize that the utility of GVL as a pulping solvent and the final portfolio of bio-based products might depend on the specific needs of the biorefinery.

2. Materials and methods

2.1. Materials

Pulping: GVL (≥99 wt%), sulfuric acid (95–97.0 wt%), NaBH₄, MgSO₄*7H₂O, NaHSO₃, di(trimethylolpropane) (97%), diphenyl carbonate (99%), Xylose (≥99 wt%), activated charcoal (100 mesh particle size) were purchased from Sigma Aldrich. Ethanol (≥99.5 wt%) was purchased from Anora. *Betula Pendula* (Silver birch) wood chips were supplied by Stora Enso (Finland). The wood chips were screened according to the SCAN-CM 40:01 (7 and 13 mm) and stored at −20 °C. NaOH pellets (99.2%), H_2O_2 (30%), and Na_2CO_3 (99.8%) were purchased from VWR. Ionic liquid (1,5-diazabicyclo[4.3.0]non-5-enium acetate) was synthesized by the combination of acetic acid (glacial, 100% for analysis; Merck, Germany) and 1,5-diazabicyclo[4.3.0]non-5-ene (DBN; Fluorochem Ltd.)in a reactor at 70 °C [28,29].

Afilan CVS and Leomin PN for spin finish were purchased from Archroma. Priamine™ 1074 for polyhydroxyurethane production was purchased from Croda GmbH. Pure sodium silicate for fabric bleaching was purchased from Merck.

Lignin NMR: Deuterated chloroform (CDCl₃), pyridine, deuterated dimethyl sulfoxide (DMSO-*d₆*), endo-*n*-hydroxy-5-norbornene-2,3-dicarboximide (e-HNDI), chromium (III) acetylacetonate (Cr(acac)₃), 2-chloro-4,4,5,5-tetramethyl-1,3,2-dioxaphospholane (TMDP) and trioxane were purchased from Sigma-Aldrich.

2.2. Acid-catalyzed fractionation of Betula pendula chips – production of fully bleached pulp

The series of acid-catalyzed GVL/H_2O fractionations at liquor-to-wood ratio (L: W) of 10 L/kg, 120 min, and 150 °C were performed

in a 10 L reactor built by the Aalto University CHEM workshop. 500 g of wood was steamed (500 g of steam) directly in the reactor, and subsequently pulped in GVL/H_2O liquor (45–65 wt% GVL) with the addition of H_2SO_4 (6–12 kg/t_{odw}). At the end of the fractionation, the raw spent liquor was discharged, and cooked wood was $2\times$ washed with 2 L of 50 wt% ethanol at 30 °C for 15 min. The pulp was disintegrated in the mixer and screened for the rejects in a table-top screener (G.A. Serlachius A.B., Model 16140-567, with a mesh opening of 0.35 mm). Screened and homogenized pulp was subjected to oxygen delignification (10% consistency) in the air bath digester (Haato Oy, Finland) equipped with 2.5 L Teflon-coated autoclaves. The delignification conditions were: 90 min, 95 °C, 7 bar O_2, 40 kg NaOH/t_{odp}, and 5 kg MgSO$_4$/t_{odp}.

The L: W ratio was further reduced to 4 while keeping constant 55 wt% of GVL with added H_2SO_4 (6–12 kg/t_{odw}). 1200 g of chips were cooked following the same procedure as for L: W = 10. After discharging the raw spent liquor, the chips were washed $2\times$ with 2.4 L of 45 wt% GVL solution. The washing GVL solution was combined with the raw spent liquor and referred to as spent liquor. The pulps followed the same one-step delignification process as pulps produced at L: W = 10. Further, only the pulp selected for fiber spinning was subjected to two-step oxygen delignification (OO), acidification (A), and ozone bleaching (Z). The conditions for oxygen delignification were: 1) 90 °C, 15 min, 25 kg NaOH/t, 8 bar O_2, 0.2 g NaBH$_4$/kg$_{odp}$; 2) 110 °C, 60 min, 15 kg NaOH/t, 8 bar O_2. The acidification was done at 1% consistency and room temperature by the addition of 1 M H_2SO_4 (pH 2–3). The conditions for ozone bleaching were: 4.5 kg O_3/t_{odp} followed by acidification step (10 g NaOH/kg$_{odp}$, 8 g H_2O_2/kg$_{odp}$, 2 g MgSO$_4$/kg$_{odp}$ at 80 °C, 180 min, and 10% consistency).

2.3. Fiber production and fabric knitting

Selected bleached pulp (Table S1, entry 15b) was spun to regenerate cellulosic fibers according to the Ioncell® process. Before pulp dissolution, [DBNH][OAc] was liquefied at 70 °C. The spinning dope was then prepared in a vertical kneader by mixing air-dried bleached GVL pulp with [DBNH][OAc] with a pulp consistency of 13 wt%. The mixture was kneaded for 2 h at 80 °C and 30 rpm at reduced pressure ($\approx$10 mbar). The resulting solution was filtered by a hydraulic press filter device (metal filter mesh with 5 μm absolute fineness, Gebr. Kufferath AG, Germany) at 80 °C to remove undissolved substrate which would lead to unstable spinning. The dope was then shaped into the dimension of the spinning cylinder and solidified at 4 °C.

Filament spinning was carried out by a customized laboratory piston spinning system (Fourné Polymertechnik, Germany) as described by Ma et al. (2018) [30]. The solidified dope was loaded in the cylinder and then heated to 80 °C to form a highly viscous, air-bubble-free spinning dope. The molten solution was extruded through a 200-hole spinneret (capillary diameter of 100 μm and a length-to-diameter ratio (L/D) of 0.2) to a 0.5 cm air gap, and subsequently, the filaments were coagulated in a water bath (10 °C). The regenerated filaments were guided by Teflon rollers to the godet couple. The extrusion velocity (V_e) was set to 5.5 ml/min (3.5 m/min) while the take-up velocity (V_t) of the godet varied from 3.5 to 39 m/min. The draw ratio (DR) is calculated as DR = V_t/V_e. The spun fibers were washed off-line in hot water (ca. 60 °C) and air-dried.

The air-dried fibers were spin finished for 5 min at 50 °C using an aqueous mixture of Afilan CVS (0.667 g/L) and Leomin PN (0.222 g/L) (liquor ratio 1:20). After the treatment, the fibers were pressed to reach 300% pick-up. The air-dried fibers were carded (Carding Machine 337A, Mesdan, Italy) and the carded fiber web was rolled into a sliver. It was drafted in a draw frame (Stiro Roving Lab 3371, Mesdan, Italy), doubled, drafted, and doubled again to elongate and homogenize the sliver. The doubled sliver was drafted in the draw frame and formed into a false-twist roving. It was ring-spun (Rin Lab 82BA, Sermates, Italy) into a 20-tex (tex = g/1000 m) yarn (Nm 50) having a Z-torsion and 700 twists per meter. The linear density of the spun yarn was determined from 10-m skeins (n = 8), and it was expressed in tex.

Finally, the spun yarn was plied into a 2-ply yarn with S-torsion and 300 twists per meter, and it was weft knitted (Stoll CMS ADF 32W E7.3 multi-gauge) into a small demonstration fabric (the square mass of knitted fabric was 115 g/m^2). The fabric was bleached (Linitest, Original Hanau, Germany) at 90 °C for 2 h with the liquor-to-fabric ratio of 1: 20. The bleaching solution consisted of 30% hydroxy peroxide (1.5 g/L), sodium silicate (7 g/L), NaOH (0.5 g/L), NaCO3 (1.8 g/L) and water. The bleached fabric was rinsed in lukewarm water, air-dried, and finished by steaming.

2.4. Lignin isolation, characterization, and polyhydroxyurethane production

Lignin was precipitated from the spent liquor (SL) by the addition of water in the ratio 1:1. The mixture was well mixed and centrifuged for 15 min at 10000 rpm (relative centrifugal force 3000 g). The supernatant was collected and stored for subsequent GVL recovery. Precipitated lignin pellets were dissolved in 5 ml of acetone and diluted with 45 ml of deionized water directly in vials. The mixture was again centrifuged, the supernatant discarded, and the lignin pellets were washed $2\times$ with 45 ml deionized water. Lignin was dried overnight in a vacuum oven at 40 °C and stored.

The polyhydroxyurethane containing lignin precipitated from SL (GVL-PHU) was prepared according to the protocol published by Zhao et al. (2021) [31]. The bis(6-membered cyclic carbonate) (BCC) was synthesized from 10 g of di(trimethylolpropane) and 85.7 g of diphenyl carbonate at 140 °C for 48 h. 1 g of synthesized BCC was mixed with 1.77 g of the dimer fatty diamine (Priamine™ 1074) and lignin (10–30 wt%). The prepared mixture was cured in the oven at 120 °C for 30 min. Subsequently, the cured mixture was processed in a hot press (SM 16276, Carver Laboratory Press, Sartorius AG, Germany) at 120 °C and 4 MPa for 5 h using a steel mold.

2.5. Xylose crystallization

Xylose solubility in a synthetic mixture containing GVL, H_2O, lignin, and xylose (69 wt%) was monitored by focused beam

reflectance measurement (FBRM) (ParticleTrack G400, Mettler Toledo, U.S.) with measuring range 0.5–2000 μm. FBRM enabled tracking the particle size and particle counts change in situ. The mixture was gradually heated up until complete particle dissolution was observed by FBRM and kept at this temperature (Table S10, $T_{saturation}$) for 1 h to verify that no crystals are formed.

Cooling crystallization of xylose was performed in a 100 ml reactor (EasyMax 420, Mettler Toledo, U.S.) with a stirring speed of 400 rpm. The composition of synthetic raffinate (Table S10) for xylose crystallization was determined and calculated based on the analysis of SL and raffinate collected after the GVL extraction combined with ASPEN data. Firstly, the mixture was heated to saturation temperature (80 °C or 85 °C) depending on its composition (Table S10) and kept for 20 min to ensure complete dissolution of xylose. Afterward, the crystal-free solution was gradually cooled to 25 °C at a constant crystallization time of 12 h (cooling rate 0.076 and 0.083 °C/min). The xylose seeds (1% of the theoretical crystal yield) were added when the solution temperature dropped 1.5 °C from the initial saturation temperature (supersaturation of solution). The crystallized xylose was separated from the mother liquor by filtration (particle retention filter paper 12–15 μm) and washed with 500 g of 90 wt% ethanol and 500 g of 100% ethanol. The xylose crystallization yield was gravimetrically determined after overnight drying.

2.6. GVL recovery by CO₂ extraction

The GVL recovery by compressed liquid CO_2 was carried out using both the synthetic solution and spent liquor produced during the fractionation (Table S2, entry 15). The composition of the synthetic solution was based on the approximate composition of spent liquor consisting of 200 g GVL, 200 g water, 1.6 g furfural, 1.6 g formic acid, and 1.6 g acetic acid. Prior to the GVL extraction from spent liquor, the lignin was precipitated by water (described in Section 2.4). The excess water in the lignin-lean spent liquor was removed by rotavapor to concentrate the GVL back to ≈50 wt% (further referred to as feed).

Before extraction, the feed was loaded into a high-pressure JERFI feed cylinder where a piston without the stem separated the feed and the water (hydraulic fluid). The liquid CO_2 was loaded into the ISCO 1000 syringe pump, which pushed liquid CO_2 into the extractor from the bottom during the run. The extraction started by filling the extractor gradually with compressed CO_2 until the liquid level reached 2 cm from the top of the extractor. After that, the turbine was turned on and the feed started to flow in by pushing it into the extractor from the top of the sapphire cell by ISCO 500 syringe pump. The volumetric rates of CO_2 and feed were predetermined and kept in constant flow mode. The magnetic-driven Oldshue-Rushton type turbine (700 rpm) inside the extraction column broke the droplets of the dispersed phase. The CO_2-rich phase (extract composed of GVL, gaseous CO_2, and furfural) was withdrawn from the top of the extractor.

The flow of the extract and the pressure of the extraction column were regulated with the Equilibar B6R Series Blockage Resistant Back Pressure Regulator (backpressure was regulated by N_2). The flash took place inside the Equilibar, consequently, the liquid GVL was collected in an Erlenmeyer flask and gaseous CO_2 was captured by the fume extraction arm. The mass flow of liquid extract was measured with an electrical scale. The raffinate was withdrawn from the bottom of the extractor and collected in the raffinate cylinder. The flow of the raffinate was regulated by the withdrawal of the high-pressure raffinate cylinder. The water (acting as a hydraulic fluid of a raffinate cylinder) was withdrawn into the ISCO 260 syringe pump. The raffinate rate was calculated before the experiments but fine-tuned visually and volumetrically using the ISCO syringe pump in refill constant flow mode. The samples of extract and raffinate were collected in 30 min intervals through six-port VICI sampling valves with the sample loop. A sample was flashed into the pressure vessel where CO_2 was determined based on the pressure increase. The composition of the liquid phase was determined by gas chromatography (GC) analysis. The duration of experiments typically took 6 h to consume all feed and to reach a steady state.
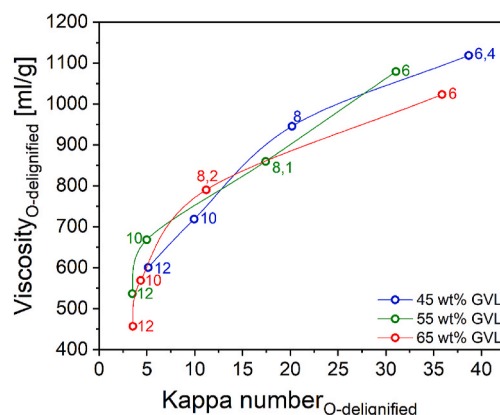
Fig. 2. Pulping selectivity of oxygen-delignified pulps for the cooks with L: W = 10 at different GVL concentrations. The digits in the graph represent the H_2SO_4 concentration in kg/t (more details in Table S1).

3. Results and discussion

3.1. Acid-catalyzed fractionation of Betula pendula chips

The results from our previous research (acid-catalyzed GVL fractionation of birch sawdust) indicated that moderate temperature (150 °C) and lower acid charges (<10 kg H_2SO_4/t_{odw}) can yield high-purity pulp [32]. As a continuation, the acid-catalyzed GVL pulping of birch at selected conditions was upscaled to a 10 L reactor. The chips were pulped firstly at a higher liquor-to-wood ratio (L: W = 10) with varying GVL and H_2SO_4 concentrations. The residual lignin in the pulp was further removed by one-step oxygen delignification. The kappa number and viscosity linearly decreased as the acid concentration increased; however, if the concentration of H_2SO_4 exceeded 10 kg/t, the viscosity exponentially dropped while the kappa number remained almost unchanged (Fig. 2). Although the lignin removal was better with a higher GVL charge at a given H_2SO_4 concentration due to the higher delignification strength of GVL, the difference in delignification selectivity was relatively small for applied GVL concentration (Fig. 3). The macro-molecular properties of oxygen-delignified pulps were well preserved at the whole range of acidic concentrations without excessive degradation of cellulosic chains closely resembling the properties of commercial dissolving pulps (Table S1).

The liquor-to-wood ratio was further reduced to aim toward potential industrial conditions. Since the pulping selectivity at a higher liquor-to-wood ratio was not prominent at any of the GVL concentrations, the subsequent experiments were conducted at a constant 55 wt% GVL as a compromise between the delignification activity of GVL and hydrolytic activity of water. Similar to results at L: W = 10, the H_2SO_4 concentration above 10 kg/t did not promote better delignification (Fig. 4). The yield loss after the pulping was low with well-preserved cellulose although the viscosity gradually dropped because of increased acidic cleavage of glycosidic bonds (Fig. 5). After detailed analysis of oxygen-delignified pulps produced at L: W = 4, we selected the pulp produced with 10 kg H_2SO_4/t (Table S1, entry 15) as the pulping conditions were sufficient to obtain a high yield (44.4% odw) and pure cellulose (89% odp) with low hemicellulose and lignin content (<5% odw).

The selected pulp was subjected to the OO-A-Z-P bleaching sequence, yielding a pulp with an ISO brightness of 90%, while the kappa number was reduced below 0.5 (Table S1, entry 15b). Although the viscosity of dissolving pulp is slightly higher than the typical values (450–500 ml/g), it is well within acceptable specifications. Higher viscosity enables slightly more intensive bleaching. On the other side, high hemicellulose content on oven-dried pulp (>8% odp) might cause difficulties in fiber spinning as well as worsened fiber properties.

3.2. Valorization of pulping streams

3.2.1. Fiber production and fabric knitting

The fully bleached GVL-water pulp (Table S1, entry 15b) was used to produce regenerated cellulose fibers. The prepared spinning solution (dope) with 13 wt% pulp solution in [DBNH][OAc] showed excellent spinnability at 85 °C. Due to the relatively low dynamic moduli at the cross-over point (COP) (1598 Pa, Table S3), which can be attributed to the relatively broad molecular mass distribution, the dope could only be spun smoothly at this higher temperature, which meant that the target values for zero shear viscosity could not be achieved. Lower temperatures led to instability during spinning due to the loss of elasticity of the spinning solution (Table S3). At a spinning temperature of 85 °C, a draw ratio of 11 could be achieved, resulting in fibers with a linear density of ~1.3 dtex, which is the fiber thickness required for textile applications.

The tenacity of Ioncell fibers is generally superior to any other fibers [24]. The same pattern was achieved with GVL-IONCELL fibers (Table 1). Despite the lower tenacity of GVL-IONCELL fibers compared to Ioncell fibers produced from pre-hydrolysis kraft (PHK) pulp, GVL-IONCELL fibers were stronger than the commercial viscose or NMMO- lyocell fibers. However, the elongation of GVL-IONCELL fibers was the lowest among all fibers, making the fibers the least elastic. The slightly inferior properties of GVL-IONCELL fibers are most likely the consequence of a high amount of non-cellulose components in the starting material. This excess of hemicelluloses (8%
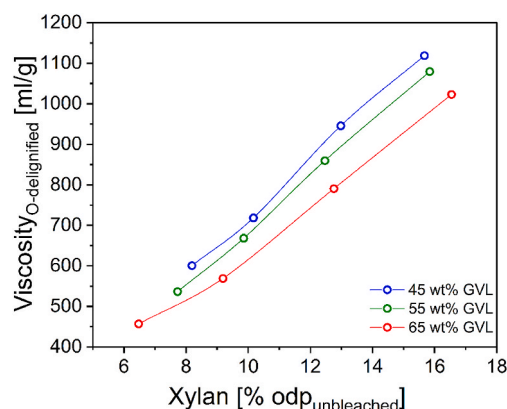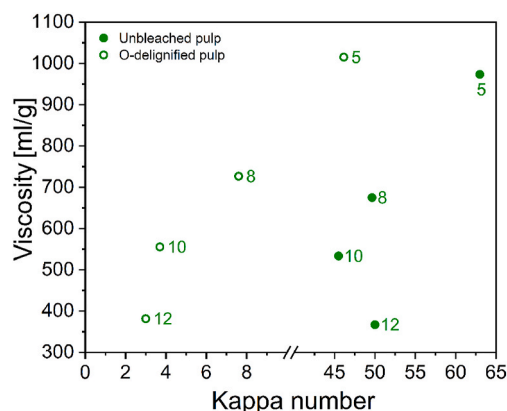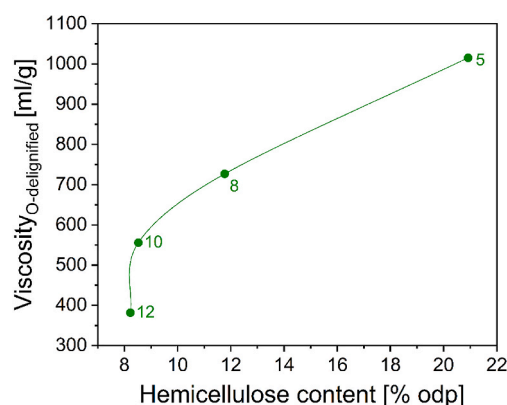

Fig. 3. Hemicellulose removal in pulps produced at L: W = 10, varying GVL and H_2SO_4 concentration (more details in Table S1).

Fig. 4. Difference in delignification selectivity before and after oxygen delignification for the cooks with L: W = 4 and 55 wt% GVL. The digits in the graph represent the H_2SO_4 concentration in kg/t (more details in Tables S1 and S2).

Fig. 5. Hemicellulose removal in pulps produced at L: W = 4, 55 wt% GVL, and varying H_2SO_4 concentration. The digits in the graph represent the H_2SO_4 concentration in kg/t (more details in Table S1).

odp, Table S1) led to disruption of the fiber orientation and consequently to the reduction of the mechanical properties. The birefringence value indicates the high orientation of cellulose molecules in GVL-IONCELL fibers.

The GVL-IONCELL yarn spinnability is fully comparable to the fibers from commercial pulp and the mechanical properties of yarn follow the same model as fibers. Because of the lower strength of fiber, the GVL-IONCELL yarn tenacity and elongation at break are lower compared to Ioncell yarn spun from commercial dissolving pulp (Table S4). Nevertheless, the strength realization of yarn (yarn tenacity/fiber tenacity) is 62%, the same as in our previous study where yarn was produced from commercial dissolving pulp [33].

Despite the high whiteness of the dissolving pulp, the washed and dried GVL-IONCELL fibers took on a reddish-yellowish hue (Table S5, Fig. S2). The formation of chromophores in the ppm range during the spinning process could be the cause of the slight coloration of the fibers, which was, however, significantly reduced by a mild peroxide treatment. The mechanism of the color formation could not be elucidated within the scope of this work. It could also be due to impurities in the pulp, in the spinning bath, or in the solvent.

3.2.2. Lignin isolation, characterization, and polyhydroxyurethane production

The first step was to isolate lignin from spent liquor (Table S2, entry 15) by the simple addition of water to induce precipitation. Lê et al. (2016) evaluated the lignin precipitation from GVL spent liquor at different SL: H_2O ratios concluding that the precipitation yield (>60% of lignin) does not improve above SL: H_2O > 2 [17]. Our experiments confirmed the same trend. Since the lignin-lean SL was further used for GVL recovery, additional water removal was needed for the reconcentration of GVL (more on this in Section 3.3). Therefore, the lignin was precipitated at an SL: H_2O ratio of 1 to avoid removing large amounts of water from the diluted lignin-lean SL. After the washing and drying, 70% of dissolved lignin (11 wt% on odw) with an average molecular weight of 4.8 kDa was collected. Thorough washing is crucial because the precipitated lignin contains residues such as GVL or carbohydrates, which lead to a viscous mixture that makes it difficult to purify the lignin (Fig. S3).

GVL-lignin had a higher content of aliphatic hydroxyl groups than Alcell™ (hardwood organosolv lignin) lignin, while the content of total phenolic hydroxyl groups and –COOH was lower compared to Alcell™ (Table S7). Low amounts of aliphatic OH, oxygenated

Table 1

Summary of linear density and mechanical properties in the conditioned and wet state, birefringence value Δn, and total orientation f_{total} of regenerated fibers.

Sample	Linear density [dtex]	conditioned test				wet test				birefringence		Reference
		Tenacity [cN/tex]	Elongation [%]	Young's modulus [GPa]	Modulus of toughness [MPa]	Tenacity [cN/tex]	Elongation [%]	Young's modulus [GPa]	Modulus of toughness [MPa]	Δn	f_{total}	
Viscose	1.80±0.10	20.70±1.50	19.20±2.20	6.90±0.50	–	7.50±1.30	16.50±1.30	–	–	0.026 ±0.003	0.42 ±0.05	[24]
NMMO-type Lyocell	1.58	34.42±4.98	13.41±2.52	–	–	–	–	–	–	–	–	[34]
IONCELL Birch PHK dissolving pulp (DR12)	1.21±0.14	49.90±4.35	12.47±1.99	–	–	47.32±4.47	14.23±2.07	–	–	0.040 ±0.005	0.65 ±0.09	[33]
IONCELL Birch PHK dissolving pulp (DR 11)	1.30±0.14	50.50±3.50	–	21.80±4.5	–	45.70±4.2	–	4.30±0.46	–	–	–	[35]
GVL-IONCELL eucalyptus bleached fibers (DR15)	1.30±0.20	41.20±3.40	10.0±1.20	17.50	–	34.70±2.4	11.0±0.6	–	–	–	–	[17]
GVL-IONCELL bleached fibers (DR11)	1.21±0.12	40.75±2.17	11.84±1.39	12.26±3.49	41.14±6.59	35.37±2.91	13.85±2.07	1.63±1.13	40.14±8.49	0.043 ±0.004	0.68 ±0.07	–

aliphatic moieties in general and β-*O*-4 (and resinol) units specifically, high amount of phenolic OH, saturated aliphatic, high degree of condensation as compared with native hardwood lignins [36] indicate that GVL-lignin is significantly degraded. This is in sharp contrast to previous claims about the "native-like" nature of GVL-lignin [37]. GVL-lignin also has a relatively high amount of carbohydrates, apparently due to the co-precipitation of hemicellulose (as compared to other hardwood organosolv lignins). The number of β-*O*-4 linkages is about the same as in Alcell™ (Table S9), although GVL-lignin is somewhat more condensed than Alcell™ despite the higher S/G ratio in GVL-lignin. The slightly higher content of the oxygenated aliphatic moieties in GVL-lignin is likely due to the contribution of the residual carbohydrates. Since the GVL-lignin structure resembles the Alcell™ lignin pattern [38], except for the lack of ethylated moieties in GVL in contrast to Alcell™, GVL-lignin could be considered for industrial applications that are appropriate for Alcell™.

The application of lignin discussed in this paper proposes using GVL-lignin as a polyol in polyurethane. The synthesis of polyurethanes is based on the exothermic reaction of polyisocyanates (-NCO) with polyols (-OH) forming urethane linkages and polyurethane network. The latest advances in polyurethane synthesis employ biobased polyols such as lignin to replace fossil-based ones [39,40]. Preparation of the GVL-polyhydroxyurethane (GVL-PHU) sample followed the protocol of Zhao et al. (2021) [31]; however, due to technical limitations, the sample was hot-pressed in a steel mold at 120 °C (Fig. S4). The elasticity of the resultant GVL-PHU did not exceed 120% for the sample containing 10% lignin and with increasing lignin content, the elasticity gradually dropped with simultaneous tensile strength increase (Fig. 6, Table S6). The FTIR measurement (Fig. S5) indicates the complete reaction of BCC with Priamine by the disappearance of the BCC characteristic peak located at 1736 cm^{-1}, which indicates the presence of carbonyl groups [31]. Further, the defined peak at 3318 cm^{-1} attributed to –OH stretching vibrations suggests lignin conversion due to the reduced intensity difference in compliance with the –CH stretching vibrations located at 2918/2854 cm^{-1} in comparison to only lignin. The thermal properties of GVL-PHU (30% lignin) were investigated by thermogravimetric analysis under a gas flow of Helium (70 ml/min) (Fig. 7) and compared with the results achieved by Ref. [31]. The degradation can be described by two major steps, the breakage of urethane bonds in combination with the degradation of lignin (300–400 °C) and the collapse of ether bonds (400–500 °C). Due to the presence of lignin, the degradation starts at around 120 °C. However, the GVL-PHU shows a great stability and reaches a T_{max} of 440 °C, which is close to the value described by Zhao et al. (2021) (447 °C) [31].

3.2.3. Xylose crystallization

In our proposed biorefinery concept based on GVL fractionation of birch wood, we propose to crystallize the separated C$_5$ hemicellulose as xylose, which is mainly contained in the raffinate (fraction after GVL recovery from SL, described in section 3.3). Under the applied conditions, only small amounts of furfural are produced, which favors the direct isolation of the xylose. Crystallization is a widely used separation process that gives highly pure products with minimal operating costs and energy demands. Cooling crystallization is based on the decreased solubility of the compound with the decreasing temperature in a controlled manner from the initial to the final temperature [41].

After GVL extraction from spent liquor, the raffinate was composed mostly of water and dissolved sugars. However, residual lignin, and a small amount of GVL and organic acids were still present. The presence of GVL and lignin might have adverse effects on xylose crystallization. The residual lignin could cause plugging of the equipment or difficulties in xylose recovery because of lignin precipitation and formation of incrustations [42]. Residual GVL could inhibit the crystallization if the xylose solubility is favored. The lignin could be readily removed by adsorption on activated carbon (Fig. S8), but the removal of small amounts of GVL detected in the raffinate is rather complicated. Therefore, we studied the influence of GVL on xylose crystallization.

Due to the insufficient amount of raffinate after the extraction (≈200 ml), it was not technically feasible to use the raffinate for xylose crystallization but instead a synthetic mixture was used. The composition of the synthetic mixture was determined based on composition analysis of spent liquor and raffinate combined with Aspen modeling. Adopting the protocol from Ferreira et al. (2014), the concentration of the xylose in a synthetic mixture was set to a constant 69 wt% [43]. The GVL content in all mixtures was kept constant at 11.6 wt% and only the residual lignin and water content varied.
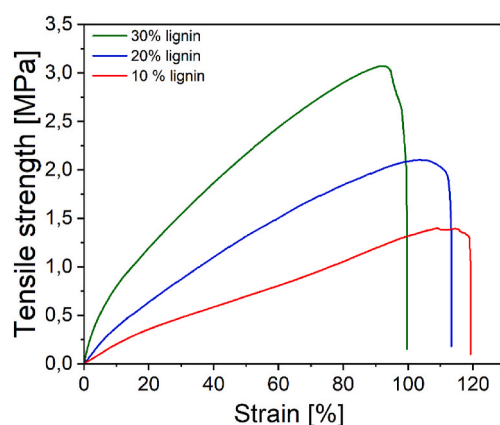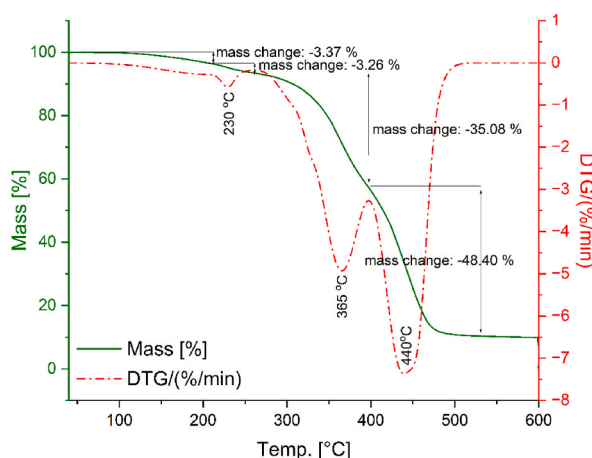

Fig. 6. Mechanical properties of GVL-PHU prepared with lignin isolated from SL after GVL fractionation.

Fig. 7. Thermal properties of GVL-PHU with 30% lignin: (green) thermogravimetry (TG) curve and (red) differential TG curve. (For interpretation of the references to color in this figure legend, the reader is referred to the Web version of this article.)

Firstly, we evaluated the solubility of xylose as a function of temperature and varying GVL and lignin composition. The dissolution was monitored by FBRM (focused beam reflectance measurement), which enabled to track the particle size and particle counts change in situ. The xylose solubility decreased as GVL concentration increased; therefore, to completely dissolve xylose, the saturation temperature had to be increased up to 85 °C at the given composition (Table S10). Once the saturation temperature was determined, the crystallization was carried out at a constant cooling time of 12 h and a final temperature of 25 °C. The overall xylose yield (>60 wt %) was increasing with higher GVL concentration (Table S10). Therefore, it could be assumed that GVL acts as an antisolvent reducing the solubility of xylose. Despite the residual GVL in raffinate would enhance the xylose crystallization, it needs to be stressed that the
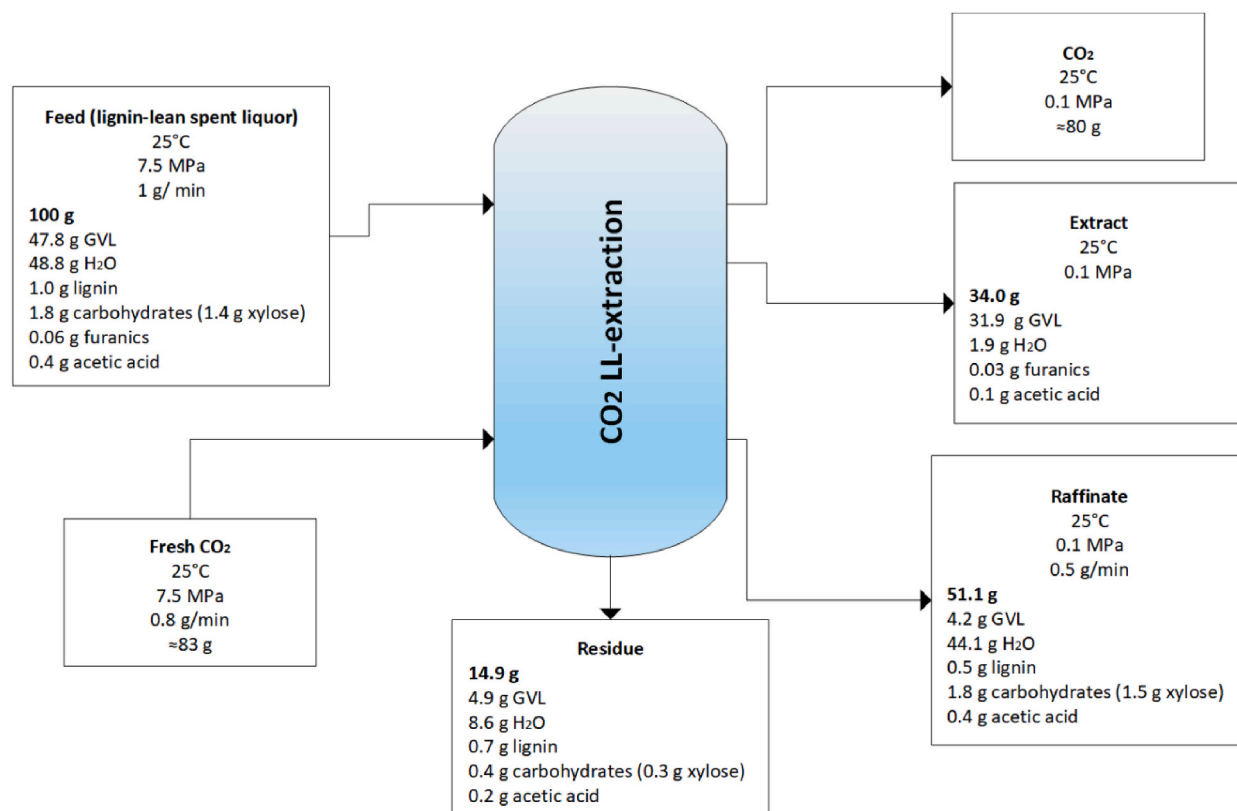
Fig. 8. Experimental GVL recovery from spent liquor produced during silver birch pulping. The extraction conditions were 26 °C, 75 MPa, and continuous feeding mode. The mass balance is based on analytical results of individual streams and calculated based on 100 g of feed.
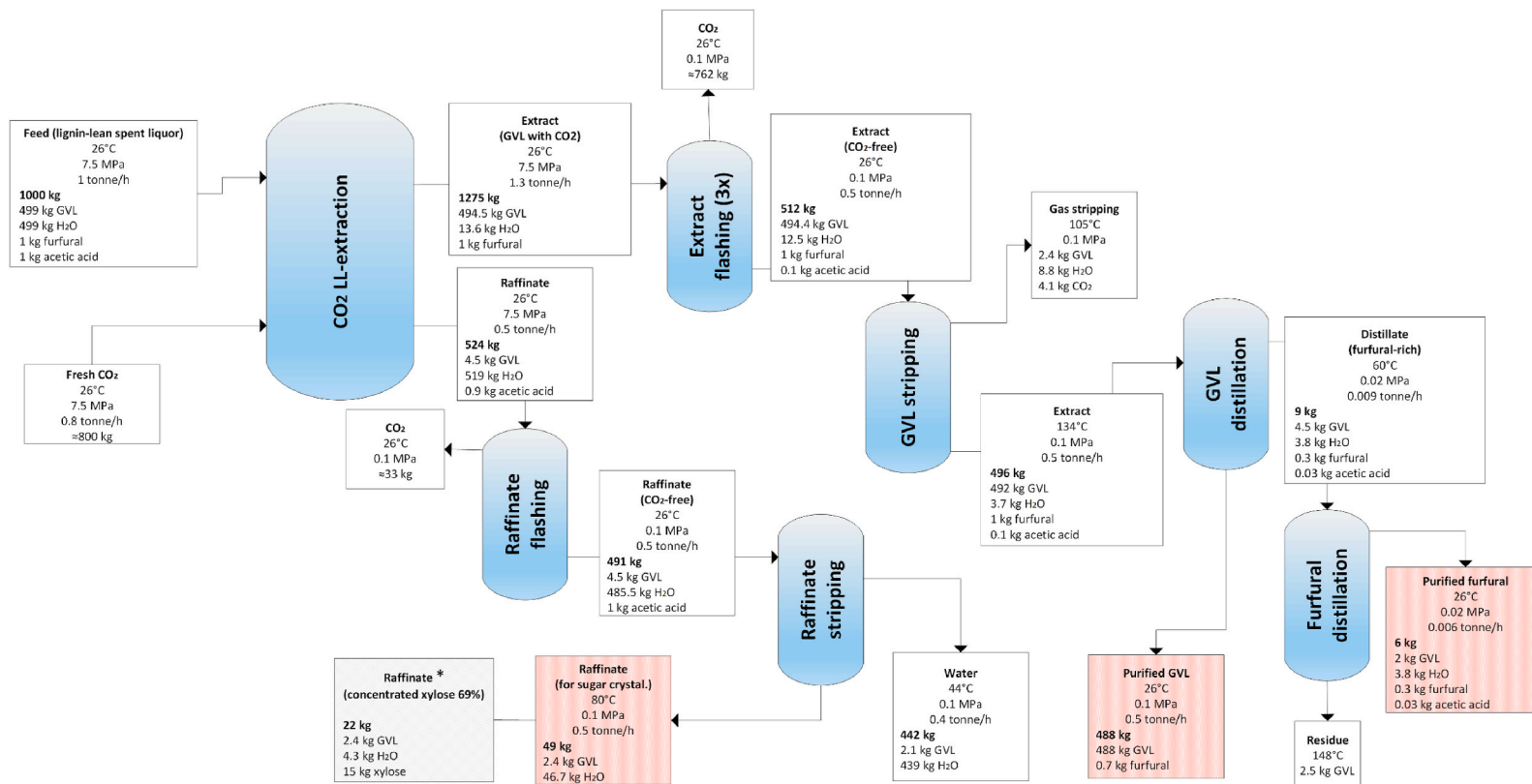
Fig. 9. Simplified scheme of GVL recovery simulated in Aspen. The mass balance is calculated based on 1000 kg of feed. The Raffinate* (gray box) represents the mass balance including xylose, which was not implemented in the Aspen simulation. The pink boxes represent the main streams of recovery. (For interpretation of the references to color in this figure legend, the reader is referred to the Web version of this article.)

GVL losses in raffinate must be minimized. Similarly, the residual lignin showed inert behavior as it can be removed by activated carbon or easily dissolved during the washing of xylose with ethanol. Although mother liquor entrapped between crystals can be washed out by ethanol resulting in pure xylose crystals (no residual GVL detected in crystals), GVL influences the formation and size of crystals (Figs. S9 and S10). The purity of crystallized xylose was not affected due to the absence of other sugars in synthetic mixture, which are usually present in spent liquor.

3.3. GVL recovery by CO$_2$ extraction

3.3.1. Experimental GVL recovery in continuous mode

In our previous research, Lê et al. (2018) demonstrated that up to 87% of GVL could be recovered as the extract in semi-batch mode through CO$_2$ extraction, while approximately 10% of GVL remained in the raffinate. Although the preliminary evaluation implied that GVL extraction by CO$_2$ is a mild and energetically self-sufficient treatment, further optimization of the process was advised [18]. Therefore, this research switched from semi-batch feeding mode to continuous mode and implemented the mixing mechanism focusing on the quantitative recovery of GVL.

After lignin precipitation, the lignin-lean diluted spent liquor (≈25 wt% GVL) (further referred to as feed) was reconcentrated to the original GVL concentration (≈50 wt% GVL) to avoid excessive CO$_2$ consumption. The feed and CO$_2$ were continuously fed into the extractor (1 g/min and 0.8 g/min, respectively), while the extract (organic gaseous phase) was discharged from the extractor by flashing down to atmospheric pressure. The raffinate (aqueous liquid phase) was continuously discharged from the extractor (0.5 g/min) but its collection had to be closely monitored. The extraction was stopped once the feed was completely consumed (≈330 g, 6 h). The residual lignin in the feed did not cause substantial problems during the extraction such as pipeline clogging. Most of the GVL could be recovered (67%) almost as a pure fraction (Fig. S11) but minor amounts of acetic acid, furfural and water present in the extract are unavoidable (Fig. 8). Nevertheless, the GVL can be purified by distillation in later stages. Approximately 9% of GVL was lost in the raffinate and the rest of GVL remained as the residue in the extractor at the end of extraction. GVL is chemically stable but during the reactions small amount of GVL hydrolyzes to 4-hydroxyvaleric acid (4-HVA), which remains mostly in the raffinate due to its affinity toward aqueous phase. Although 4-HVA is present in both, extract and raffinate, it is unclear to what degree its presence influences GVL recovery. The raffinate was composed mostly of water, dissolved sugars, small amounts of lignin, and residual GVL.

Although the laboratory column operated in the counter-current flow mode, a significant loss of GVL was observed. The reason for this is the fact that there are only three real separation stages with relatively small column height. The estimated stage efficiencies were approximately 30%.

3.3.2. Simulation of GVL recovery

An Aspen model was validated based on the laboratory experiments (section 3.3.1). Further, the model was based on PC-SAFT equation of state with validated interaction parameters for the present system, and a liquid-liquid extractor model built into the Aspen flowsheet simulator (Tables S11, S12, S13).

By assuming 10 ideal stages for the process, 99% of GVL could be recovered from the feed (Fig. 9); however, a small amount of GVL loss during the CO$_2$ release (extract flashing) and GVL purification results in a total of 98% of recovered GVL that could be recycled back to pulping digester. Furfural is extracted from the feed together with GVL and it can be separated during GVL distillation (Fig. 9). Furfural-rich distillate can be further treated to obtain approximately 30% of purified furfural in one recovery cycle. Nevertheless, furfural distillation is energetically demanding and its complete separation from acetic acid is challenging.

Around 1% of GVL is lost in the raffinate, which is further treated in a stripping column to remove excess water (Fig. 9). The water removed from the raffinate can be reused in the digester (Fig. S12) and therefore, a small amount of GVL is recycled together with the water as well. As a result, 0.5% GVL (from the original GVL amount in the feed) remains in the raffinate.

Although the GVL fraction in the raffinate is considered to be a loss of solvent, its presence significantly enhances the xylose isolation. The Aspen software does not consider xylose in simulation but it is assumed that dissolved xylose remains in the raffinate due to low volatility. Therefore, the mass balance of GVL recovery (Fig. 9, gray box) estimates the composition of raffinate including the xylose (concentrated sugar solution).

The estimated mass balance of the whole process (Table S16) implies that more than 51% of the original wood could be converted to products (37% fibers, 9.3% polyhydroxyurethane, 4.4% xylose, and 0.1% furfural) following the proposed protocol without any optimization of the GVL-H$_2$O fractionation process.

To reduce the energy consumption of GVL recovery, mechanical vapor recompression and a three-stage compressor for CO$_2$ compression were proposed (Table S17). However, the detailed energy balance including biomass pulping, lignin, and xylose isolation is required to determine the energetical self-sufficiency of the mill.

4. Conclusion

The continued research in GVL as a solvent for birch wood fractionation confirms the great potential of GVL to become the green solvent of the future. In this paper, we proposed for the first time a complete GVL biorefinery concept in which all polymeric wood fractions from one pulping sequence were exemplarily recycled into textile fibers, polyhydroxyurethane, and xylose after GVL/water pulping under optimized conditions. The presented work contains detailed characterization of wood by-products and valorized products. Additionally, for the first time we evaluated the novel GVL recovery by CO$_2$ recovery in continuous mode and the results were verified by extensive Aspen simulation.

The fully bleached pulp obtained after the GVL water cooking process and subsequent TCF bleaching resembled the properties of a commercial acid sulfite pulp, only the hemicellulose content was slightly higher due to the lack of hot alkali extraction as used in commercial dissolving pulp production. Nevertheless, the pulp was successfully spun into IONCELL fibers with good strength values and further processed into yarn and a high-quality knitted fabric.

70% of the lignin in the birch wood could be isolated after precipitation by adding water and most of it could be converted into a thermostable polyhydroxyurethane as a valuable material.

The hemicellulose fraction removed from the birch wood could be isolated from the raffinate with high yield as pure xylose by cooling crystallization. It could be demonstrated that the presence of GVL in the raffinate had no negative influence on the crystallization yield.

The GVL recovery in the laboratory column was 66% due to the limited number of equilibrium stages. As confirmed by Aspen modelling, the GVL yield can be increased to 99% if the number of equilibrium stages is increased to ten.

Funding

Declaration of competing interest

The authors declare that they have no known competing financial interests or personal relationships that could have appeared to influence the work reported in this paper

Acknowledgments

Appendix A. Supplementary data

Supplementary data to this article can be found online at https://doi.org/10.1016/j.heliyon.2023.e17423.

References

[1] United Nations, Climate Action and Synergies https://sdgs.un.org/topics/climate-change (accessed 16 February 2023).
[2] IPCC, in: O. Edenhofer, R. Pichs-Madruga, Y. Sokona, E. Farahani, S. Kadner, K. Seyboth, A. Adler, I. Baum, S. Brunner, P. Eickemeier, B. Kriemann, J. Savolainen, S. Schlömer, C. von Stechow, T. Zwickel, J.C. Minx (Eds.), Climate change 2014: mitigation of climate change, Contribution of Working Group III to the Fifth Assessment Report of the Intergovernmental Panel on Climate Change, Cambridge University Press, Cambridge, United Kingdom and New York, NY, USA, 2014.
[3] H. Sixta, Part I 1 Chemical pulping, in: H. Sixta (Ed.), Handbook of Pulp, 2006, pp. 2–19.
[4] R. Alén, Biorefining of forest resources, in: R. Alén (Ed.), Papermaking Science and Technology - Book 20, Paper Engineers' Association, Helsinki, 2011, pp. 56–114.
[5] A.A. Shatalov, H. Pereira, Polysaccharide degradation during ozone-based TCF bleaching of non-wood organosolv pulps, Carbohydr. Polym. 67 (2007) 275–281.
[6] T.N. Kleinert, K. Tayenthal, Über neuere Versuche zur Trennung von Cellulose und Inkrusten Verschiedener Hölzer, Angew. Chem. 44 (1931) 788–791.
[7] J. Sundquist, Organosolv pulping, in: J. Gullichsen, C.-J. Fogelholm (Eds.), Papermaking Science and Technology - Book 6B Chemical Pulping, Fapet Oy, Jyväskylä, 2000, pp. 411–427.
[8] J.J. Bozell, S.K. Black, M. Myers, D. Cahill, W.P. Miller, S. Park, Solvent fractionation of renewable woody feedstocks: organosolv generation of biorefinery process streams for the production of biobased chemicals, Biomass Bioenergy 35 (2011) 4197–4208.
[9] M. Iakovlev, T. Pääkkönen, A. van Heiningen, Kinetics of SO 2-ethanol-water pulping of spruce, Holzforschung 63 (2009) 779–784.
[10] Chempolis, Technologies & Solutions. https://chempolis.com/technologies-solutions/. (Accessed 16 February 2023).
[11] Fortum, Bio2X: high-value products from biomass https://www.fortum.com/products-and-services/biobased-solutions/bio2x (accessed 16 February 2023).
[12] I.T. Horváth, H. Mehdi, V. Fábos, L. Boda, L.T. Mika, γ-Valerolactone-a sustainable liquid for energy and carbon-based chemicals, Green Chem. 10 (2008) 238–242.
[13] D.M. Alonso, J.M.R. Gallo, M.A. Mellmer, S.G. Wettstein, J.A. Dumesic, Direct conversion of cellulose to levulinic acid and gamma-valerolactone using solid acid catalysts, Catal. Sci. Technol. 3 (2013) 927–931.
[14] M. Granatier, I. Schlapp-Hackl, H.Q. Lê, K. Nieminen, L. Pitkänen, H. Sixta, Stability of gamma-valerolactone under pulping conditions as a basis for process optimization and chemical recovery, Cellulose 28 (2021) 11567–11578.
[15] J.S. Luterbacher, J.M. Rand, D.M. Alonso, J. Han, J.T. Youngquist, C.T. Maravelias, B.F. Pfleger, J.A. Dumesic, Nonenzymatic sugar production from biomass using biomass-derived γ-valerolactone, Science 343 (2014) 277–280.
[16] W. Fang, H. Sixta, Advanced biorefinery based on the fractionation of biomass in γ-valerolactone and water, ChemSusChem 8 (2015) 73–76.
[17] H.Q. Lê, Y. Ma, M. Borrega, H. Sixta, Wood biorefinery based on γ-valerolactone/water fractionation, Green Chem. 18 (2016) 5466–5476.
[18] H.Q. Lê, J.P. Pokki, M. Borrega, P. Uusi-Kyyny, V. Alopaeus, H. Sixta, Chemical recovery of Î-valerolactone/water biorefinery, Ind. Eng. Chem. Res. 57 (2018) 15147–15158.
[19] D.M. Alonso, S.H. Hakim, S. Zhou, W. Won, O. Hosseinaei, J. Tao, V. Garcia-Negron, A.H. Motagamwala, M.A. Mellmer, K. Huang, C.J. Houtman, N. Labbé, D. P. Harper, C.T. Maravelias, T. Runge, J.A. Dumesic, Increasing the revenue from lignocellulosic biomass: maximizing feedstock utilization, Sci. Adv. 3 (2017) 1–7.

[20] M.A. Talebi, G.R. Dick, Y.M. Questell-Santiago, J.S. Luterbacher, Fractionation of lignocellulosic biomass to produce uncondensed aldehyde-stabilized lignin, Nat. Protoc. 14 (2019) 921–954.

[21] Statista,Projected production capacity of chemical pulp worldwide from 2020 to 2025 (in 1,000 metric tons)*, https://www.statista.com/statistics/871672/production-capacity-chemical-pulp-forecast-worldwide/(accessed 16 February 2023).

[22] A. Engelhardt, The Fiber Year 2022, 2022.

[23] S. Shokri, S. Hedjazi, H.Q. Lê, A. Abdulkhani, H. Sixta, High-purity cellulose production from birch wood by γ-valerolactone/water fractionation and IONCELL-P process, Carbohydr. Polym. 288 (2022), 119364.

[24] A. Michud, M. Tanttu, S. Asaadi, Y. Ma, E. Netti, P. Kääriainen, A. Persson, A. Berntsson, M. Hummel, H. Sixta, Ioncell-F: ionic liquid-based cellulosic textile fibers as an alternative to viscose and Lyocell, Text, Res. J. 86 (2016) 543–552.

[25] L.P. Christopher, Integrated forest Biorefineries: current state and development potential, in: L.P. Christopher (Ed.), Integrated Forest Biorefineries Challenges and Opportunities, RSC Green Chemistry, Croydon, UK, 2013, pp. 1–66.

[26] D.S. Bajwa, G. Pourhashem, A.H. Ullah, S.G. Bajwa, A concise review of current lignin production, applications, products and their environment impact, Ind. Crops Prod. 139 (2019), 111526.

[27] Statista,Market value of polyurethane worldwide from 2015 to 2021, with a forecast for 2022 to 2029, https://www.statista.com/statistics/720449/global-polyurethane-market-size-forecast/(accessed 16 February 2023).

[28] H. Sixta, A. Michud, L. Hauru, S. Asaadi, Y. Ma, A.W.T. King, I. Kilpeläinen, M. Hummel, Ioncell-F: a high-strength regenerated cellulose fibre, Nord. Pulp Pap. Res. J 30 (2015) 43–57.

[29] L.K.J. Hauru, M. Hummel, A. Michud, H. Sixta, Dry jet-wet spinning of strong cellulose filaments from ionic liquid solution, Cellulose 21 (2014) 4471–4481.

[30] Y. Ma, M. Hummel, I. Kontro, H. Sixta, High performance man-made cellulosic fibres from recycled newsprint, Green Chem. 20 (2018) 160–169.

[31] W. Zhao, Z. Liang, Z. Feng, B. Xue, C. Xiong, C. Duan, Y. Ni, New kind of lignin/polyhydroxyurethane composite: green synthesis, smart properties, promising applications, and good reprocessability and recyclability, ACS Appl. Mater. Interfaces 13 (2021) 28938–28948.

[32] M. Granatier, H.Q. Lê, C.E. González, H. Sixta, Birch Fractionation in γ-valerolactone with the Emphasis on Pulp Properties: Prehydrolysis, Acid-Catalyzed, and Alkaline-Catalyzed Concept, RSC Sustain, 2022.

[33] S. Haslinger, Y. Ye, M. Rissanen, M. Hummel, H. Sixta, Cellulose fibers for high-performance textiles functionalized with incorporated gold and silver nanoparticles, ASC Sustainable Chem. Eng. 8 (2019) 649–658.

[34] Y. Ma, M. Rissanen, X. You, K. Moriam, M. Hummel, H. Sixta, New method for determining the degree of fibrillation of regenerated cellulose fibres, Cellulose 28 (2021) 31–44.

[35] W. Fang, E. Sairanen, S. Vuori, M. Rissanen, I. Norrbo, M. Lastusaari, H. Sixta, UV-sensing cellulose fibers manufactured by direct incorporation of photochromic minerals, ASC Sustainable Chem. Eng. 9 (2021) 16338–16346.

[36] M.Y. Balakshin, E.A. Capanema, R.B. Santos, H.M. Chang, H. Jameel, Structural analysis of hardwood native lignins by quantitative 13C NMR spectroscopy, Holzforschung 70 (2016) 95–108.

[37] L. Shuai, M.T. Amiri, Y.M. Questell-Santiago, F. Héroguel, Y. Li, H. Kim, R. Meilan, C. Chapple, J. Ralph, J.S. Luterbacher, Formaldehyde stabilization facilitates lignin monomer production during biomass depolymerization, Science 354 (2016) 329–334.

[38] M.Y. Balakshin, E.A. Capanema, Comprehensive structural analysis of biorefinery lignins with a quantitative 13 C NMR approach, RSC Adv. 5 (2015) 87187–87199.

[39] P. Furtwengler, L. Avérous, Renewable polyols for advanced polyurethane foams from diverse biomass resources, Polym. Chem. 9 (2018) 4258–4287.

[40] H. Li, Y. Liang, P. Li, C. He, Conversion of biomass lignin to high-value polyurethane: a review, J. Bioresour. Bioprod. 5 (2020) 163–179.

[41] K. Pal, Y. Yang, Z.K. Nagy, Model-based optimization of cooling crystallization of active pharmaceutical ingredients undergoing thermal degradation, Cryst. Growth Des. 19 (2019) 3417–3429.

[42] J.S. Gütsch, H. Sixta, Purification of Eucalyptus globulus water prehydrolyzates using the HiTAC process (high-temperature adsorption on activated charcoal), Holzforschung 65 (2011) 511–518.

[43] J.A. Ferreira, C.O. Teixeira, S.M. Soares, Process for the Production of Crystalline Xylose from Sugar Cane Bagasse, Crystalline Xylose Obtained by Said Process, Process for the Production of Xylitol from the Said Xylose and Crystalline Xylitol Obtained Thereby, 2004, US20060281913A1.